International Journal of Power Electronics and Drive Systems (IJPEDS)
Vol. 15, No. 4, December 2024, pp. 2058~2067
ISSN: 2088-8694, DOI: 10.11591/ijpeds.v15.i4.pp2058-2067

Single observer speed sensorless field weakening control of two parallel motors

Agus Suprajitno, Feri Yusivar, Abdul Halim
Faculty of Engineering, Department of Electrical Engineering, Universitas Indonesia (UI), Jakarta, Indonesia

Article Info

Article history:

Received Mar 12, 2024
Revised Aug 26, 2024
Accepted Sep 5, 2024

Keywords:

Field weakening
Induction motor
Nominal speed
RFOC
Single observer

ABSTRACT

Two induction motors with parallel connected stator windings supplied by a single inverter (single observer) with a field weakening control system. The objective of this study is to propose a torque production speed sensorless vector control technique for each parallel connected rotor by adding field weakening control to improve the performance of each motor and reducing the number of adaptive observers on each motor to a single observer. Design of a rotor flux-oriented control (RFOC) system. Simulation results with the C-MEX S-function of MATLAB/Simulink 2015b show that the proposed method works better and can be operated at speeds that exceed the nominal speed of the motor.

Corresponding Author:

Feri Yusivar
Faculty of Engineering, Department of Electrical Engineering, Universitas Indonesia
UI Depok Campus, Jakarta, 16424 Indonesia
Email: yusivar@eng.ui.ac.id

1. INTRODUCTION

Industry uses induction motors with cage rotors extensively due to their robust design and affordable cost in comparison to other motors of the same class. In use, a speed adjustment is required to control the set point or the desired speed, and then a feedback system is required, which is rotor speed information. Two methods were used to collect the rotor speed information: sensor-based and speed-sensorless. In systems with sensors, the use of encoders often cannot detect very low and very high speeds. To overcome this problem, a sensorless speed control system is designed by applying current vector control to control and estimate the rotor speed, which is fed back to the system [1]-[8]. Induction motors can be precisely driven by a single inverter running a single induction motor by the use of the field-oriented control approach of sensorless vector control. On the other hand, a single inverter can power several induction motors connected in parallel for industrial uses such electric propulsion, as in railroad traction systems [9], [10]. Due to hardware minimization and cost reduction, multiple induction motors, considered one large motor, can be driven by a single inverter under the same specifications and rating. However, when an uneven load torque is applied, the performance becomes unstable [11].

Control with field weakening is one method to improve the performance of induction motors. With this method, speeds that can exceed the nominal speed can be achieved. S.H. Kim and S.K. Sul used field weakening in maximum torque operations [12], Briz *et al.* [13] used current and voltage regulation to achieve revolutions above nominal revolutions. Kerkman *et al*. using indirect field-oriented control in the application of field weakening [14]. In this research, the motor rotation is estimated with an observer on the ab-axis reference frame using the motor flux weakening control or field weakening control method while taking into account the limits of the motor nominal voltage and current so that the motor rotation can be achieved beyond the nominal rotation with maximum torque operation, and the stability of the motor rotation is determined by the Lyapunov stability theory.

In general, sensorless induction motors are controlled in parallel without field weakening control. The number of observers in induction motor parallel control is directly correlated with the number of motors; hence, the more motors under control, the greater the number of observers. Numerous observers necessitate intricate mathematical computations, which are laborious to complete. In order to minimize this problem from multiple observers to one, a creative mathematical calculation incorporating multiple observers is required. In this study, the field weakening method is applied to parallel two induction motors to obtain better performance. What distinguishes the parallel of induction motors in the previous study (two observers) is that the observer is only one piece. The proposed method is applied to a 0.75 HP (0.55 kW) induction motor drive system.

2. RESEARCH METHOD

2.1. Mathematical modeling

2.1.1. Induction motor model

The induction motor model used is three phases. To simplify the calculation and analysis, a Clarke transformation is used, which converts the current, voltage, and flux equations of the three phases to the form of two stationary phases, or α-β axes. In matrix form, it can be expressed as (1).

$$\begin{bmatrix} i_\alpha \\ i_\beta \\ i_0 \end{bmatrix} = \sqrt{\frac{2}{3}} \begin{bmatrix} 1 & -\frac{1}{2} & -\frac{1}{2} \\ 0 & -\frac{1}{2}\sqrt{3} & \frac{1}{2}\sqrt{3} \\ \frac{1}{2} & \frac{1}{2} & \frac{1}{2} \end{bmatrix} \begin{bmatrix} i_a \\ i_b \\ i_c \end{bmatrix} \tag{1}$$

The Park transformation is used to transform a stationary two-phase axis to a rotating two-phase axis or direct-quadrature - dq axis, which is expressed by (2).

$$\begin{bmatrix} i_d \\ i_q \end{bmatrix} = \begin{bmatrix} \cos\theta_e & \sin\theta_e \\ -\sin\theta_e & \cos\theta_e \end{bmatrix} \begin{bmatrix} i_\alpha \\ i_\beta \end{bmatrix} \tag{2}$$

The motor model is designed in the frame of reference for stator currents on the dq axis and rotor fluxes. The general equation of an induction motor is as (3) to (6) [15].

$$\bar{V}_s = R_s \bar{\imath}_s + \frac{d}{dt}\bar{\psi}_s + j\omega_e \bar{\psi}_s \tag{3}$$

$$\bar{V}_r = R_r \bar{\imath}_r + \frac{d}{dt}\bar{\psi}_r + j(\omega_e - \omega_r)\bar{\psi}_r \tag{4}$$

$$\bar{\psi}_s = L_s \bar{\imath}_s + L_m \bar{\imath}_r \tag{5}$$

$$\bar{\psi}_r = L_r \bar{\imath}_r + L_m \bar{\imath}_s \tag{6}$$

The (3) to (6) are derived to obtain the induction motor model on the αβ axis. In reference to the stator frame $\omega_e = 0$ and the rotor being a cage rotor type, the rotor voltage Vr is zero, and the actual motor model is expressed in (7) to (10) as [16], [17]:

$$\frac{d}{dt} i_{s\alpha} = \left(-\frac{R_s}{\sigma L_s} - \frac{(1-\sigma)}{\sigma \tau_r}\right) i_{s\alpha} + \frac{L_m}{\sigma L_s L_r \tau_r}\psi_{r\alpha} + \frac{L_m \omega_r}{\sigma L_s L_r}\psi_{r\beta} + \frac{1}{\sigma L_s} V_{s\alpha} \tag{7}$$

$$\frac{d}{dt} i_{s\beta} = \left(-\frac{R_s}{\sigma L_s} - \frac{L_m^2}{\sigma L_s L_r \tau_r}\right) i_{s\beta} - \frac{L_m \omega_r}{\sigma L_s L_r}\psi_{r\alpha} + \frac{L_m}{\sigma L_s L_r \tau_r}\psi_{r\beta} + \frac{1}{\sigma L_s} V_{s\beta} \tag{8}$$

$$\frac{d}{dt}\psi_{r\alpha} = -\frac{R_r}{L_r}\psi_{r\alpha} + \frac{R_r}{L_r} L_m i_{s\alpha} - \omega_r \psi_{r\beta} \tag{9}$$

$$\frac{d}{dt}\psi_{r\beta} = -\frac{R_r}{L_r}\psi_{r\beta} + \frac{R_r}{L_r} L_m i_{s\beta} - \omega_r \psi_{r\alpha} \tag{10}$$

The stator voltage equation on the dq axis is as (11) and (12).

$$v_{sd} = R_s i_{sd} + \sigma L_s \frac{d}{dt} i_{sd} - \sigma L_s \omega_e i_{sq} + \frac{L_m^2}{L_r} \frac{d}{dt} i_{mr} \quad (11)$$

$$v_{sq} = R_s i_{sq} + \sigma L_s \frac{d}{dt} i_{sq} - \sigma L_s \omega_e i_{sd} + \frac{L_m^2}{L_r} \omega_e i_{mr} \quad (12)$$

The flux model gives the magnitude and angular position of the rotor flux and torque expressed in the (13)-(16).

$$\frac{d}{dt} i_{mr} = \frac{R_r}{L_r} (i_{sd} - i_{mr}) \quad (13)$$

$$\omega_e = N_p \omega_r + \frac{R_r}{L_r} \frac{i_{sq}^*}{i_{mr}} \quad (14)$$

$$\frac{d}{dt} \theta_e = \omega_e \quad (15)$$

$$T_e = N_p (1 - \sigma) L_s i_{sq} i_{mr} \quad (16)$$

2.1.2. Design of controllers

In (17), the speed controller is represented as an integrator proportional (IP) regulator. Since the IP controller is just as simple as the PI controller, but offers superior performance, that is why we went with it [18]. The speed controller output is finite, and when it reaches this limit, the integration start value in the next iteration is reset to the integration start value in the previous iteration to prevent the stopping phenomenon.

$$T_e^* = K_{spi} \int (\omega_r^* - \omega_r^{\wedge}) dt - k_{spp} \omega_r^{\wedge} \quad (17)$$

Values with a "*" sign indicate reference values, and values with a "^" sign indicate estimated values. The field weakening controller aims to weaken the field, but the stator current and voltage remain within the maximum current and voltage limits. The current and voltage limit equations are expressed in (18) and (19) [12].

$$v_{sd}^{*2} + v_{sq}^{*2} \leq V_{smax}^2 \quad (18)$$

$$i_{sq}^{*2} + i_{sd}^{*2} \leq I_{smax}^2 \quad (19)$$

"Field weakening" is done by controlling the d-axis stator reference current and providing a maximum q-axis stator reference current limit, as shown in Figure 1. The field weakening controller equations can be expressed in (20) and (21) [19].

$$i_{sd}^* = K_i \int (V_{s\,max}^2 - V_s^2)\, dt + K_p (V_{s\,max}^2 - V_s^2) \quad (20)$$

$$i_{sq\ limiter}^* = \sqrt{I_{s\,max}^2 - i_{sd}^2} \quad (21)$$

The current vector controller used is PI, but this controller can only control linear systems, so in (11) and (12) must be linearized using decoupling as in equations (22) to (25) [16], [17], [20].

$$v_{sd} = u_{sd} + v_{cd} \;\; v_{sq} = u_{sq} + v_{cq} \quad (22)$$

$$u_{sd} = R_s i_{sd} + L_s \sigma \frac{d}{dt} i_{sd} \;\; u_{sq} = R_s i_{sq} + L_s \sigma \frac{d}{dt} i_{sq} \quad (23)$$

$$v_{cd} = -\omega_e L_s \sigma i_{sq} + L_s (1 - \sigma) \frac{d}{dt} i_{mr} \quad (24)$$

$$v_{cq} = \omega_e L_s \sigma i_{sd} + L_s (1 - \sigma) \omega_e i_{mr} \quad (25)$$

With v_{cd} and v_{cq} being the coupling voltages, u_{sd} and u_{sq} are the stator voltages after decoupling. Based on the voltage decoupling equation and the general formula of the PI controller as (26) and (27).

$$(R_s i_{sd} + L_s \sigma s i_{sd}) = \left(k_{idp} + \frac{k_{idi}}{s}\right) i_{sd}^* - \left(k_{idp} + \frac{k_{idi}}{s}\right) i_{sd} \quad (26)$$

$$\left(k_{idp}+\frac{k_{idi}}{s}\right)i_{sd}^{*}=i_{sd}\left(R_s+L_s\sigma s+k_{idp}+\frac{k_{idi}}{s}\right) \quad (27)$$

Using the identity method, the controller constant for the d-axis is obtained as (28).

$$k_{idp}=\frac{L_s\sigma}{T_d}\ k_{idi}=\frac{R_s}{T_d} \quad (28)$$

In the same way, it is done on the q-axis so that the controller constant for the q-axis is obtained as (29).

$$k_{iqp}=\frac{L_s\sigma}{T_d}\ k_{iqi}=\frac{R_s}{T_d} \quad (29)$$

The controller constant values obtained were found to be the same:

$$k_{idp}=k_{iqp}=k_p$$
$$k_{idi}=k_{iqi}=k_i$$

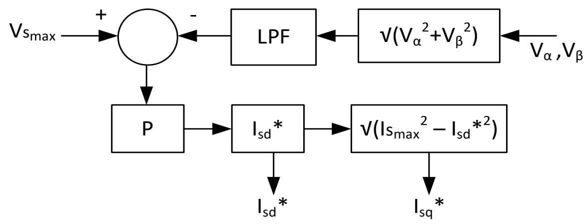

Figure 1. Field weakening controller diagram block

2.1.3. Observer in reference frame αβ

The Luenberger Observer in this design uses the αβ-axis reference frame and is made based on the induction motor model in the αβ-axis reference frame. The system model is as (30).

$$\dot{x}=Ax+Bu\ y=Cx \quad (30)$$

With *u* as the input and *y* as the output, if the system is in the estimated state, then the state and output equations become (31).

$$\dot{\hat{x}}=A\hat{x}+Bu\ \hat{y}=C\hat{x} \quad (31)$$

Matrix A is the induction motor model in the αβ axis, and its state space form is shown by the (32) and (33) [21].

$$\frac{d}{dt}\begin{bmatrix} i_{s\alpha}\\ i_{s\beta}\\ \psi_{r\alpha}\\ \psi_{r\beta}\end{bmatrix}=\begin{bmatrix} -\frac{R_s}{\sigma L_s}-\frac{(1-\sigma)}{\sigma\tau_r} & 0 & \frac{L_m}{\sigma L_s L_r\tau_r} & \frac{L_m}{\sigma L_s L_r}\omega_r\\ 0 & -\frac{R_s}{\sigma L_s}-\frac{(1-\sigma)}{\sigma\tau_r}-\frac{L_m}{L_s L_r}\omega_r & & \frac{L_m}{\sigma L_s L_r\tau_r}\\ \frac{L_m}{\tau_r} & 0 & -\frac{1}{\tau_r} & -\omega_r\\ 0 & \frac{L_m}{\tau_r} & \omega_r & -\frac{1}{\tau_r}\end{bmatrix}\begin{bmatrix} i_{s\alpha}\\ i_{s\beta}\\ \psi_{r\alpha}\\ \psi_{r\beta}\end{bmatrix}+\begin{bmatrix}\frac{1}{\sigma L_s} & 0\\ 0 & \frac{1}{\sigma L_s}\\ 0 & 0\\ 0 & 0\end{bmatrix}\begin{bmatrix}V_{s\alpha}\\ V_{s\beta}\end{bmatrix} \quad (32)$$

$$\frac{d}{dt}\begin{bmatrix} i_{s\alpha}\\ i_{s\beta}\\ \psi_{r\alpha}\\ \psi_{r\beta}\end{bmatrix}=\begin{bmatrix} a_{r11} & 0 & a_{r12} & -a_{i12}\\ 0 & a_{r11} & a_{i12} & a_{r12}\\ a_{r21} & 0 & a_{r22} & -a_{i22}\\ 0 & a_{r21} & a_{i22} & a_{r22}\end{bmatrix}\begin{bmatrix} i_{s\alpha}\\ i_{s\beta}\\ \psi_{r\alpha}\\ \psi_{r\beta}\end{bmatrix}+\begin{bmatrix} b_1 & 0\\ 0 & b_1\\ 0 & 0\\ 0 & 0\end{bmatrix}\begin{bmatrix}V_{s\alpha}\\ V_{s\beta}\end{bmatrix}$$

$$\begin{bmatrix} i_{s\alpha}\\ i_{s\beta}\end{bmatrix}=\begin{bmatrix}1 & 0\ 0 & 0\\ 0 & 1\ 0 & 0\end{bmatrix}\begin{bmatrix} i_{s\alpha}\\ i_{s\beta}\\ \psi_{r\alpha}\\ \psi_{r\beta}\end{bmatrix}$$

$$y=Cx \quad (33)$$

where $\sigma = 1 - \left(L_m^2 / L_s L_r\right)$; $\tau_r = L_r / R_r$. Use the Luenberger observer to estimate the induction motor's parameters. The following represents the (34) and (35):

$$\frac{d}{dx}\hat{x} = A\hat{x} + Bu + G(e_{is}) \tag{34}$$

$$\hat{y} = C\hat{x} \tag{35}$$

The observer feedback value is indicated by the "G" sign, whereas the estimated value is shown by the "^" sign; where,

$$\hat{x} = \begin{bmatrix} \hat{\imath}_{s\alpha} \\ \hat{\imath}_{s\beta} \\ \hat{\psi}_{r\alpha} \\ \hat{\psi}_{r\beta} \end{bmatrix}; u = \begin{bmatrix} V_{s\alpha} \\ V_{s\beta} \end{bmatrix}; e_{is} = \begin{bmatrix} e_{is\alpha} \\ e_{is\beta} \end{bmatrix}; \hat{y} = \begin{bmatrix} \hat{\imath}_{s\alpha} \\ \hat{\imath}_{s\beta} \end{bmatrix}$$

The observer model's eigenvalue is $\det\,(I\mu - (A - GC)$ and the induction motor model's eigenvalue is $\det\,(I\mu - A)$. The value of G is obtained as the observer's reinforcement feedback (37), using the derived (36).

$$|I\mu - A| = |I\lambda - (A - GC| \tag{36}$$

Then we get (37).

$$G = \begin{bmatrix} g_1 & g_2 & g_3 & g_4 \\ -g_2 & g_1 & -g_4 & g_3 \end{bmatrix}^T \tag{37}$$

Where $g_1 = (k-1)(a_{r11} + a_{r22})$, $g_2 = (k-1)a_{i22}$, $g_3 = -(k^2-1)(\lambda a_{r11} + a_{r21}) + \lambda(k-1)(a_{r11} + a_{r22})$, $g_4 = \lambda(k-1)a_{i22}$, $\lambda = (\sigma\, L_s L_r / L_m)$; $k > 0$. By computing $e_{is\beta}$ (beta stator current error) and $e_{is\alpha}$ (alpha stator current error), one may get the estimated rotor speed ($\hat{\omega}_r$). In (38) illustrates how it is derived using Lyapunov's theory [22]:

$$\hat{\omega}_r = K_p\left(\hat{\psi}_\beta e_{is\alpha} - \hat{\psi}_\alpha e_{is\beta}\right) + K_i \int \left(\hat{\psi}_\beta e_{is\alpha} - \hat{\psi}_\alpha e_{is\beta}\right) dt \tag{38}$$

Where $e_{is\alpha} = \hat{\imath}_{s\alpha} - i_{s\alpha}$ and $e_{is\beta} = \hat{\imath}_{s\beta} - i_{s\beta}$.

2.1.4. Induction motor parallel vector control

With the same motor specifications, two induction motors can be regarded as a single, huge motor. Nonetheless, the stator currents will vary if the torque loads on the motors are not balanced. Because it is used to operate two motors, the stator current that is flowing and circulating from the inverter needs to be split into two portions (i_{s1} and i_{s2}). The current flow of two induction motors operating in parallel is displayed in Figure 2.

The (39) and (40) show the average circulating current between the two motors as well as the average stator current calculated using the average and difference techniques [23]:

$$\bar{\imath}_s = (i_{s1} + i_{s2})/2 \tag{39}$$

$$\Delta\bar{\imath}_s = (i_{s2} - i_{s1})/2 \tag{40}$$

Motor 1's and Motor 2's stator currents are displayed by the variables i_{s1} and i_{s2}, respectively.

The current stator command to regulate the average torque (41) and average rotor flux (42) is obtained using the induction motor's vector model [24]-[26].

$$\bar{\imath}_{sq}^{e*} = \left((\bar{T}'^*/p\bar{M}') - \Delta\hat{\bar{\imath}}_{sd}^e \Delta\hat{\bar{\psi}}_{rd}^e + \Delta\hat{\bar{\imath}}_{sq}^e \Delta\hat{\bar{\psi}}_{rq}^e\right) / \hat{\bar{\psi}}_{rd}^{e*} \tag{41}$$

Where $\bar{T}' = (\bar{T}_e - (\Delta\bar{M}'/\bar{M}')\Delta\bar{T}_e)/(1 - (\Delta\,\bar{M}'/M')^2)$. $\bar{T}' = \bar{T}_e$ because the parameters of the two induction motors are regarded as being identical, meaning that the value of $\Delta\bar{M}'$ is zero. Where $\bar{T}_e = (T_{e1} + T_{e2})/2$.

$$\bar{\imath}_{sd}^{e*} = \left(\bar{S}_r \bar{\psi}_{rd}^{e*} + \Delta\hat{\bar{\omega}}_r \Delta\hat{\bar{\psi}}_{rq}^{e} + \Delta\bar{S}_r \Delta\hat{\bar{\psi}}_{rd}^{e} - \Delta\bar{U}\Delta\bar{\imath}_{sd}^{e}\right)/\bar{U} \quad (42)$$

Where $\bar{\psi}_r^e = \frac{(\psi_{r1}^e+\psi_{r2}^e)}{2}$; $\Delta\psi_r^e = \frac{(\psi_{r2}^e-\psi_{r1}^e)}{2}$, $\bar{\imath}_s^e = \frac{(i_{s1}^e+i_{s2}^e)}{2}$; $\Delta i_r^e = \frac{(i_{s2}^e-i_{s1}^e)}{2}$, $\bar{S}_r = \frac{(S_{r1}+S_{r2})}{2}$; $\Delta S_r = \frac{(S_{r2}-S_{r1})}{2}$, $\bar{U} = \frac{(U_1+U_2)}{2}$; $U = \frac{(U_2-U_1)}{2}$, $\bar{\omega} = \frac{(\omega_{r1}+\omega_{r2})}{2}$; $\Delta\omega = \frac{(\omega_{r2}-\omega_{r1})}{2}$, and $S_r = (R_r/L_r)$; $U = MS_r$.

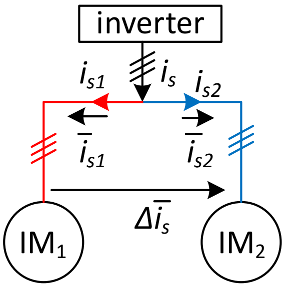

Figure 2. The current flowing through two induction motors connected in parallel

2.2. Configuration of the proposed method

Figure 3 shows the configuration of the sensorless parallel induction motor origin. An adaptive speed observer is present for every motor, as demonstrated below. The configuration of the proposed system is shown in Figure 4. The average and difference calculating mechanisms get motor current from the inverter. The voltage from the inverter and the currents produced by the average and difference processes are transformed from *abc* to *αβ*. $I_{\alpha\beta}$ and $V_{\alpha\beta}$ are the Luenberger observer's inputs after conversion. The reason for its transformation is that the observer model makes use of the stator reference frame. The motor speed, stator current, and rotor flux are all estimated by the Luenberger observer. The controller output, which acts as the inverter input, is found by subtracting the average stator current from the command average stator current.

2.3. Implementation

Disturbances of balanced and unbalanced load torque are used to show sensorless vector control using an IP speed controller. Simulations were run using MATLAB/Simulink C-Mex S-Function. The realization of the proposed parallel motor system configuration model is shown in Figure 5. The simulated nominal motor speed is 1380 rpm, or 144.5 rad/sec. The parameters are displayed in Table 1.

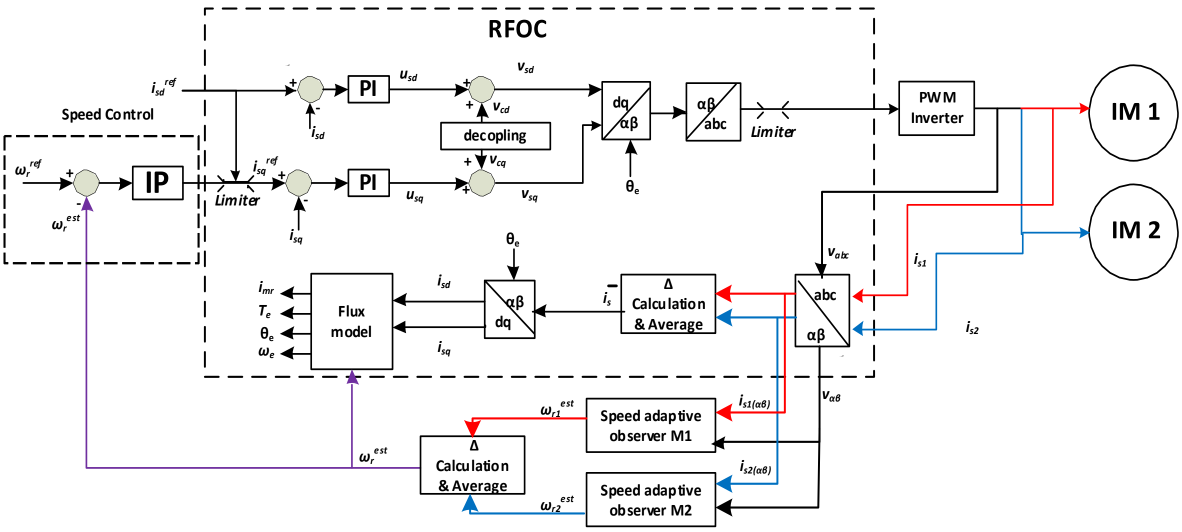

Figure 3. Parallel induction motor original configuration

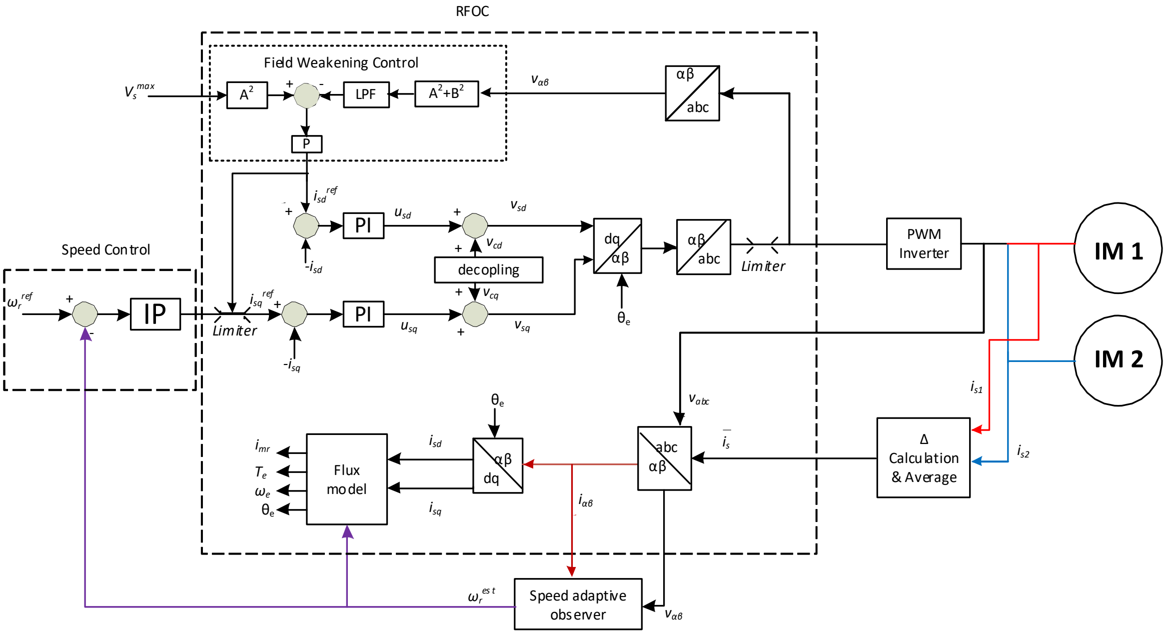

Figure 4. Configuration of the proposed system

Table 1. Induction motor parameters

Parameter	Symbol	Value	Unit	Parameter	Symbol	Value	Unit
Nominal speed motor	ω_r	1380 or 144.5	rpm or rad/s	Stator inductance	L_s	702.13	mH
Stator resistance	R_s	14.03	Ω	Rotor inductance	L_r	702.13	mH
Rotor resistance	R_r	13.29	Ω	Pole pair	N_p	2	
Mutual inductance	L_m	687.41	mH				

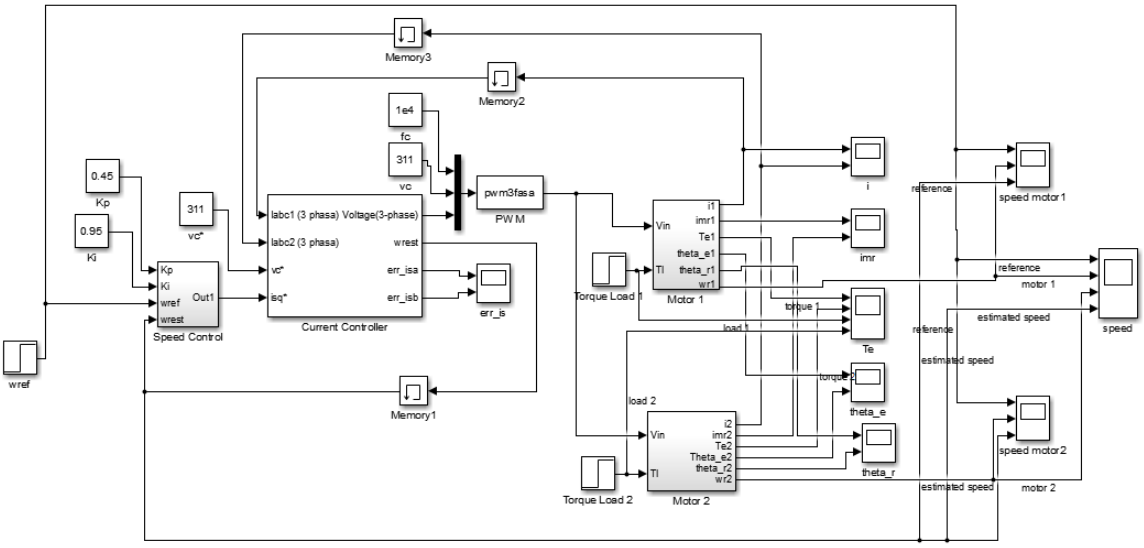

Figure 5. The realization of the proposed parallel motor system configuration model

3. SIMULATION RESULTS

The first simulation compares two observers using the suggested methodology. The second time, the motor speed command was adjusted to 100 rad/second from its initial setting of 50 rad/second as in Figure 6 (see in Appendix). Second, using the suggested method, the simulation is given a speed input of 3.46 motor nominal speed of 500 rad/second as in Figure 7. Figure 6 displays the torque step-up response simulation findings for both the two-observer approach and the suggested method. The motor speed command is set at 50 rad/second then changed to 100 rad/second at time 2 seconds. Induction motors 1 and 2 start out with no load, and after 4 and 5 seconds, they are given a 6-Nm load. As seen in Figure 6(a), each motor's torque generation can be tracked by its load. However, as Figure 6(b) demonstrates, each motor's torque generation can be adjusted in response to its load. Thus, Figure 6(c) illustrates the uniform convergence of each motor's motor speed, while Figure 6(d) illustrates the uniform convergence of each motor's motor speed, albeit with a delay towards reference.

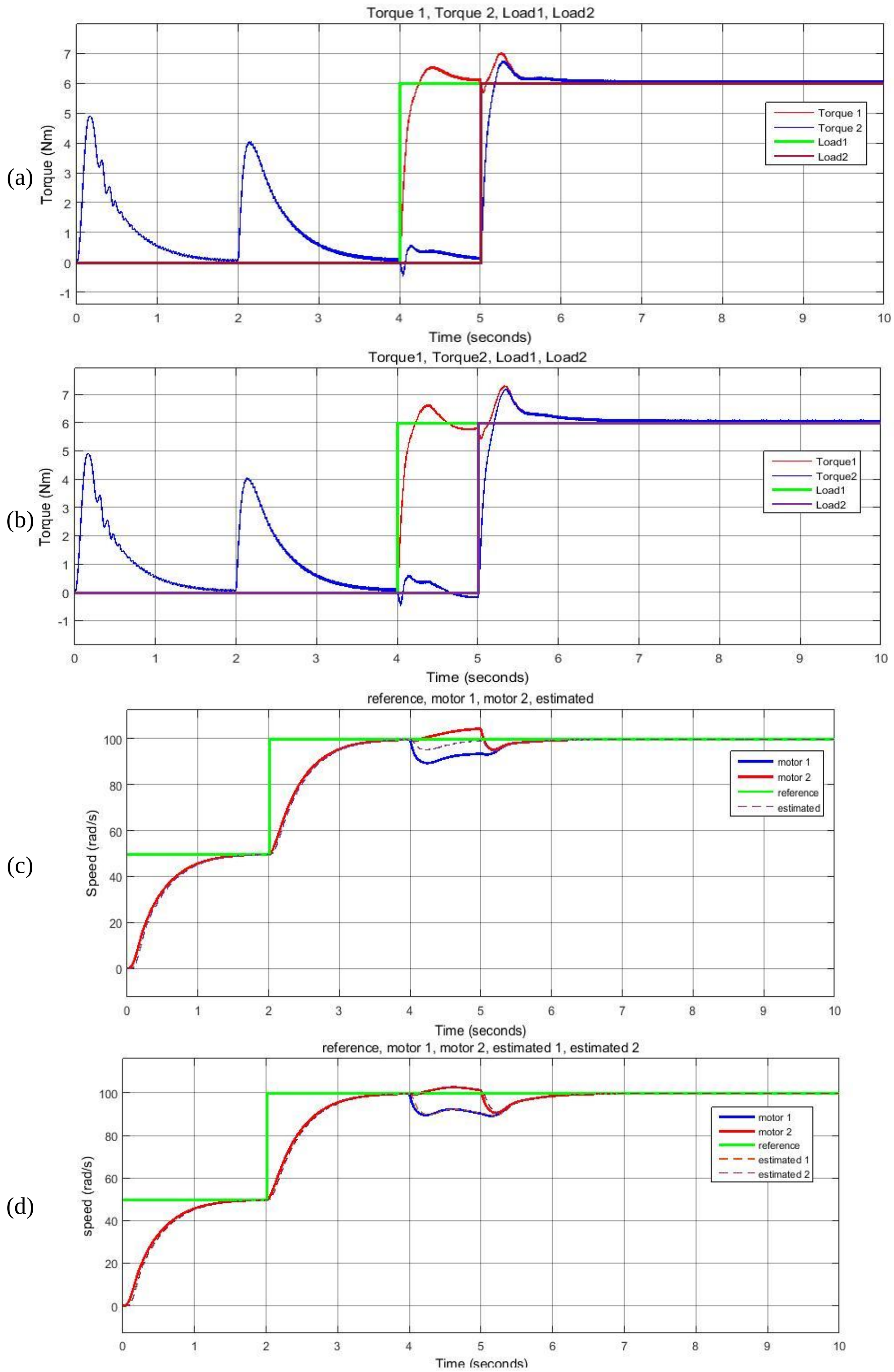

Figure 6. Simulation result for torque step-up response: (a) the suggested approach for torque response, (b) the two-observer method for torque response, (c) motor speed: suggested approach, and (d) two-observer approach for motor speed

In Figure 7, the simulation is given a speed input of 3.46 motor nominal speed of 500 rad/second. Figure 7 shows the difference in time to reach the reference value between the speed of the two motors and the estimated speed, namely that the actual speed of the motor is 0.2 seconds faster than the estimated speed when there is no load. In the simulation, both motors are given a load of 2 Nm each at different times, with motor 1 at the 6th second and motor 2 at the 7th second. At the 6th second of motor 1, there is a decrease in speed of around 493 rad/s for 1 second, and motor 2 overshoots the speed, reaching 511 rad/s at the 7th second. At the 7th second, motor 2 decreased its speed to around 505 rad/s, and at that time, motor 1 overshoot speed reached 503 rad/s. And the speed of the two motors was uniform at 503 rad/s at the 9,2 second. So that the speed of both motors exceeds the estimated speed and reference speed by 3 rad/s.

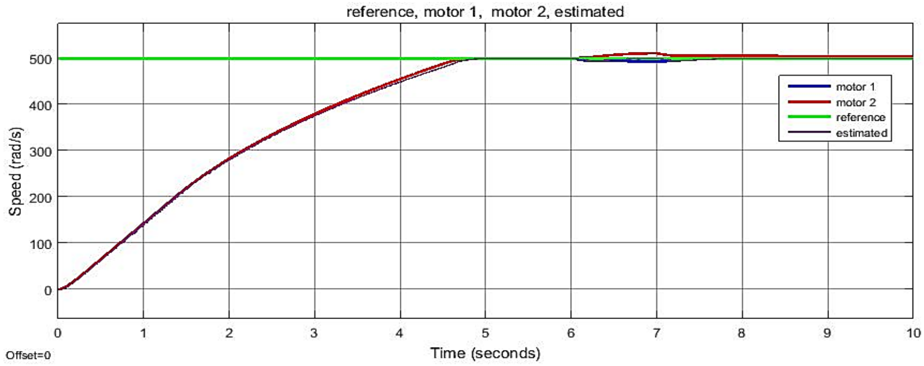

Figure 7. Response to a speed step-up: simulation's outcome motor speed using the suggested technique

4. CONCLUSION

With the addition of a "field weakening" control system, we have presented a direct field-oriented control approach for two induction motors coupled in parallel with a single observer. The "field weakening" control system can be used to adjust the rotor speed beyond its nominal speed, and for the motor used, it reaches 3.46 times the nominal speed of the motor; the error between the actual and reference speed values is 0.6%. The simulation results show that the proposed method works better and can be operated at speeds exceeding the nominal speed of the motor.

REFERENCES

[1] R. Ottersten and L. Harnefors, “Design and analysis of inherently sensorless rotor-flux-oriented vector control systems,” in *Proceding NORPIE*, Stockholm, 2002.

[2] J. Maes and J. A. Melkebeek, “Speed-sensorless direct torque control of induction motors using an adaptive flux observer,” *IEEE Transactions on Industry Applications*, vol. 36, no. 3, pp. 778–785, 2000, doi: 10.1109/28.845053.

[3] V.-. Leppanen, “Low-frequency signal-injection method for speed sensorless vector control of induction motors,” Helsinki University of Technology, 2003.

[4] L. C., B. I., and B. F., “Comparative study of adaptive and inherently sensorless observers for variable-speed induction-motor drives,” *IEEE Transactions on Industrial Electronics*, vol. 53, no. 1, pp. 57–65, 2006.

[5] G. Edelbaher, K. Jezernik, and E. Urlep, “Low-speed sensorless control of induction machine,” *IEEE Transactions on Industrial Electronics*, vol. 53, no. 1, pp. 120–129, 2006, doi: 10.1109/TIE.2005.862307.

[6] A. B. Proca, A. Keyhani, and J. M. Miller, “Sensorless sliding-mode control of induction motors using operating condition dependent models,” *IEEE Transactions on Energy Conversion*, vol. 18, no. 2, pp. 205–212, 2003, doi: 10.1109/TEC.2003.811717.

[7] M. Chenafa, A. Mansouri, A. Bouhenna, E. Etien, A. Belaidi, and M. A. Denai, “Global Stability of Linearizing Control With a New Robust Nonlinear Observer of the Induction Motor,” *International Journal of Applied Mathematics and Computer Science*, vol. 15, no. 2, pp. 235–243, 2005.

[8] A. Suprajitno and F. Yusivar, “Parallel concept of speed sensorless induction motor control,” in *AIP Conference Proceedings*, 2021, vol. 2376, doi: 10.1063/5.0065202.

[9] Y. Matsumoto, S. Ozaki, and A. Kawamura, “A novel vector control of single-inverter multiple-induction-motors drives for Shinkansen traction system,” in *Conference Proceedings - IEEE Applied Power Electronics Conference and Exposition - APEC*, 2001, vol. 1, pp. 608–614, doi: 10.1109/apec.2001.911710.

[10] F. J. Pérez-Pinal, C. Núñez, and R. Álvarez, “Multi-motor synchronization technique applied in traction devices,” *2005 IEEE International Conference on Electric Machines and Drives*, pp. 1542–1548, 2005, doi: 10.1109/iemdc.2005.195925.

[11] P. M. Kelecy and R. D. Lorenz, “Control methodology for single inverter, parallel connected dual induction motor drives for electric vehicles,” in *PESC Record - IEEE Annual Power Electronics Specialists Conference*, 1994, vol. 2, doi: 10.1109/pesc.1994.373800.

[12] S. H. Kim, “Voltage control strategy for maximum torque operation of an induction machine in the field-weakening region,” *IEEE Transactions on Industrial Electronics*, vol. 44, no. 4, pp. 512–518, 1997, doi: 10.1109/41.605628.

[13] F. Briz, A. Diez, M. W. Degner, and R. D. Lorenz, “Current and flux regulation in field-weakening operation [of induction motors],” in *Conference Record of 1998 IEEE Industry Applications Conference. Thirty-Third IAS Annual Meeting (Cat. No.98CH36242)*, 2002, vol. 1, pp. 524–531, doi: 10.1109/IAS.1998.732363.

[14] R. J. Kerkman, T. M. Rowan, and D. Leggate, "Indirect Field-Oriented Control of an Induction Motor in the Field-Weakening Region," *IEEE Transactions on Industry Applications*, vol. 28, no. 4, pp. 850–857, 1992, doi: 10.1109/28.148451.
[15] P. Vas, "Electrical machines and drives : a space-vector theory approach," in *Monographs in electrical and electronic engineering 25*, 1992, pp. xviii, 808 p.
[16] F. Yusivar and S. Wakao, "Minimum requirements of motor vector control modeling and simulation utilizing C MEX S-function in MATLAB/SIMULINK," *Proceedings of the International Conference on Power Electronics and Drive Systems*, vol. 1, pp. 315–321, 2001, doi: 10.1109/peds.2001.975333.
[17] R. Gunawan, F. Yusivar, and Z. A. Kadir, "Field Oriented Control of An Induction Motor Speed Sensorless with Current Vector Controller , direct-quadrature Current Compensator and Full Order Observer In direct-quadrature Axis," 2006.
[18] F. Yusivar, H. Haratsu, T. Kihara, S. Wakao, and T. Onuki, "Performance comparison of the controller configurations for the sensorless IM drive using the modified speed adaptive observer," in *8th International Conference on Power Electronics and Variable Speed Drives*, 2000, vol. 2000, no. 475, pp. 194–200, doi: 10.1049/cp:20000244.
[19] F. Yusivar and S. Wakao, "Field-weakening scheme combined with saturated voltage control strategy," *Proceedings of the IASTED International Conference on Modelling, Identification and Control*, vol. 23, pp. 417–422, 2004.
[20] N. A. Wicaksono, A. Halim, A. Subiantoro, and F. Yusivar, "Critical condition of sensorless induction generator using flux weakening in wind turbine application," *International Journal of Power Electronics and Drive Systems*, vol. 7, no. 1, pp. 202–216, 2016, doi: 10.11591/ijpeds.v7.i1.pp202-216.
[21] F. Yusivar, K. Uchida, H. Haratsu, S. Wakao, and T. Onuki, "Speed adaptive observer for Sensorless IM Drive using combined reference frames," *Conference Proceedings - IEEE Applied Power Electronics Conference and Exposition - APEC*, vol. 1, pp. 127–132, 2000, doi: 10.1109/apec.2000.826094.
[22] K. Azegami, T. Inoue, K. Matsuse, S. Ito, and Y. Nakajima, "Characteristics of speed sensorless vector controlled two induction motor drive fed by single inverter," *Conference Proceedings - 2012 IEEE 7th International Power Electronics and Motion Control Conference - ECCE Asia, IPEMC 2012*, vol. 4, pp. 2323–2327, 2012, doi: 10.1109/IPEMC.2012.6259216.
[23] H. Kawai, Y. Kouno, and K. Matsuse, "Characteristics of speed sensorless vector control of parallel connected dual induction motor fed by a single inverter," in *Proceedings of the Power Conversion Conference-Osaka 2002, PCC-Osaka 2002*, 2002, vol. 2, pp. 522–527, doi: 10.1109/PCC.2002.997571.
[24] G. Ramachandran, S. Veerana, and S. Padmanaban, "Vector control of a three-phase parallel connected two motor single inverter speed sensorless drive," *Turkish Journal of Electrical Engineering and Computer Sciences*, vol. 24, no. 5, pp. 4027–4041, 2016, doi: 10.3906/elk-1410-48.
[25] K. Matsuse, Y. Kouno, H. Kawai, and S. Yokomizo, "A speed-sensorless vector control method of parallel-connected dual induction motor fed by a single inverter," *IEEE Transactions on Industry Applications*, vol. 38, no. 6, pp. 1566–1571, 2002, doi: 10.1109/TIA.2002.804763.
[26] J. Nishimura, K. Oka, and K. Matsuse, "A method of speed sensorless vector control of parallel-connected dual induction motors by a single inverter with a rotor flux control," in *Proceeding of International Conference on Electrical Machines and Systems, ICEMS 2007*, 2007, pp. 600–603, doi: 10.1109/ICEMS12746.2007.4412033.

BIOGRAPHIES OF AUTHORS

Agus Suprajitno was born in Semarang, Indonesia. He received his bachelor's degree in Electrical Engineering at Universitas Islam Sultan Agung in 1998 and master's degree in Electrical Engineering at University Indonesia (UI) in 2004. He is currently an Electrical Engineering student at the Universitas Indonesia (UI) and an electrical engineering lecturer at Universitas Islam Sultan Agung. His research interests are in control system, robotic, electric drive, power electronics, and renewable energy. He can be contacted at email: agus.suprajitno@ui.ac.id.

Feri Yusivar was born in Bandung, Indonesia. He is a lecturer in Electrical Engineering Department at the Universitas Indonesia (UI), West Java, Indonesia. He received his bachelor degree in Electrical Engineering at University of Indonesia in 1992, and completed his doctor degree in 2003 at Waseda University, Japan. He is currently the head of the research center for Advanced Vehicles (RCAVe), Universitas Indonesia. His research interests are in control system, electrical drive, power electronics, and renewable energy. He can be contacted at email: yusivar@eng.ui.ac.id.

Abdul Halim was born in Jakarta, Indonesia. He is a lecturer in Electrical Engineering Department at the Universitas Indonesia (UI), West Java, Indonesia. He received his bachelor and master degree in Electrical Engineering at Keio University, Japan in 1995 and 1997, and also completed his doctor degree in 2000 at Tokyo Institute of Technology, Japan. He is currently the lecturer in Electrical Engineering at Universitas Indonesia. His research interests are in control system engineering, power system engineering, computer simulation, intelligent engineering, and applied mathematics. He can be contacted at email: a.halim@ui.ac.id.